Journal of Alloys and Compounds 509 (2011) 6834–6837

Contents lists available at ScienceDirect

Journal of Alloys and Compounds

journal homepage: www.elsevier.com/locate/jallcom

Effect of electron density on the martensitic transition in Ni–Mn–Sn alloys

R.L. Wang[a], J.B. Yan[a], H.B. Xiao[a], L.S. Xu[a], V.V. Marchenkov[b], L.F. Xu[a], C.P. Yang[a,*]

[a] Faculty of Physics & Electronic Technology, Hubei University, Wuhan, 430062, People's Republic of China
[b] Institute of Metal Physics, 620041, Ekaterinburg, Russia

ARTICLE INFO

Article history:
Received 9 February 2011
Received in revised form 13 March 2011
Accepted 19 March 2011
Available online 29 March 2011

Keywords:
Ferromagnetic shape memory alloy
Martensitic phase transition
Electron density

ABSTRACT

The structure and martensitic transition (MT) temperatures of $Ni_{44}Mn_{45}Sn_{10}R$ (R = Al, Ga, In and Sn) alloys were investigated. Valence electron concentration and cell volume are two main factors affecting the MT temperatures in Ni–Mn based Heusler alloys. Our results indicated that the MT temperatures do not vary monotonously with either of the two factors, but increase with the increasing of electron density. Combining the two factors, electron density might be a more appropriate parameter to describe the variations of MT temperatures.

1. Introduction

Since the large magnetic-field-induced strain was reported in Ni_2MnGa [1], Ni–Mn based ferromagnetic shape memory alloys (FSMAs) have attracted considerable attentions for potential applications in magnetic-field-controlled actuators and sensors. The off-stoichiometric $Ni_{50}Mn_{50-y}X_y$ (X = In, Sn and Sb) FSMAs with some critical ranges of X concentration undergo a reversible first-order martensitic transition (MT) between the high temperature austenitic phase and the low temperature martensitic phase, which is often accompanied by the sharp change in the magnetization and resistivity [2]. The reverse transition from martensitic to austenitic phase can be induced by applying magnetic field as well as increasing temperature [3]. Since the output stress originating from magnetic-field-induced phase transition is larger than that resulted from variant rearrangement in martensitic phase, the metamagnetic shape-memory alloys Ni–Mn–X (X = In, Sn, and Sb) might be more promising magnetic smart materials than conventional ferromagnetic shape-memory alloys such as Ni_2MnGa [4]. Furthermore, due to the strong coupling between structural and magnetic degrees of freedom in Ni–Mn–X (X = In, Sn, and Sb) alloys, a variety of other multifunctional properties, such as large inverse magnetocaloric effect (MCE) [5,6], giant magnetoresistance (MR) [7,8] and giant magnetothermal conductivity (MTC) [9] have been observed in the vicinity of the MT. Therefore, from viewpoint of applications, tuning the MT temperatures (including martensite start temperature M_s, martensite finish temperature M_f, austenite start temperature A_s, and austenite finish temperature A_f) and enlarging the working-temperature interval are of great importance for these FSMAs.

It is generally acknowledged that valence electron concentration, i.e. valence electrons per atom (e/a), plays a critical role in the martensitic transition of Ni–Mn based FSMAs, and in general the MT temperatures increase with the increasing of e/a [10]. Here the valence electron is calculated as the number of 3d and 4s electrons of transition metals (Ni, Mn, Co, or Cu) and the number of 5s and 5p electrons of In, Sn, or Sb. Adjusting the elemental chemical composition and partial substitution by other elements are two main methods to tune the MT temperatures. In most cases, for example, adjusting the Ni/Mn ratio [11,12], substituting Ni or Mn with Co and Cu [13,14], or replacing In with Sb [15], the variations of the MT temperatures are in accord with the valence electron concentration theory. Actually, the changes of chemical composition or alloying elements can affect not only the electronic structure but also the geometry structure. In some cases, the effect of size factor on the MT temperatures cannot be neglected and should be taken into account. For instance, isoelectronic substitution with smaller radius elements will decrease the cell volume and then results in the increasing of the MT temperatures, which was further confirmed by the experimental results in $Ni_{50}Mn_{34}In_{16-x}Ga_x$ [16] and $Ni_{43}Mn_{46}Sn_{11-x}Ge_x$ alloys [17]. Sharma et al. found that replacing Mn in $Ni_{50}Mn_{34}In_{16}$ alloy partially by smaller radius Cr with fewer valence electrons could increase the MT temperatures, indicating that the chemical pressure (size factor) effect dominates over the effect related to e/a [18].

In order to investigate the mechanism of the variations of MT temperatures in Ni–Mn–X (X = In, Sn, and Sb) alloys, in this work, a systematic substitution of III main group elements (Al, Ga and In)

* Corresponding author. Tel.: +86 27 88665447; fax: +86 27 88663390.
E-mail address: cpyang@hubu.edu.cn (C.P. Yang).

0925-8388/$ – see front matter © 2011 Elsevier B.V. All rights reserved.
doi:10.1016/j.jallcom.2011.03.128

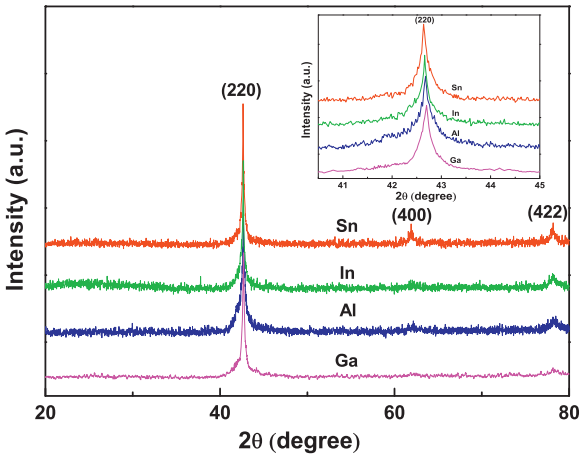

Fig. 1. The XRD patterns of $Ni_{44}Mn_{45}Sn_{10}R$ (R = Al, Ga, In and Sn) alloys at room temperature.

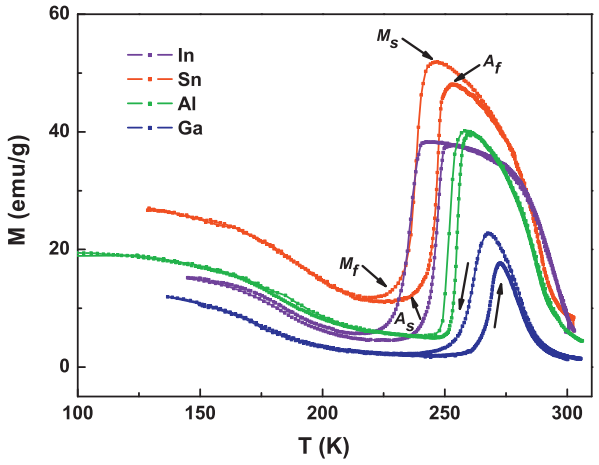

Fig. 2. The temperature dependence of magnetization for $Ni_{44}Mn_{45}Sn_{10}R$ (R = Al, Ga, In and Sn) alloys on heating and cooling under a magnetic field of 1000 Oe.

for Sn in the off-stoichiometric $Ni_{44}Mn_{45}Sn_{11}$ alloys was performed and the effects of valence electron concentration and cell volume on the variations of MT temperatures were studied in detail.

2. Experimental

The polycrystalline samples of nominal compositions $Ni_{44}Mn_{45}Sn_{10}R$ (R = Al, Ga, In and Sn) alloys were prepared by arc-melting the required amount of constituent high purity elements in a cold copper crucible under the argon atmosphere protection. The samples were flipped and re-melted several times to ensure homogeneity. The ingots were cut into small pieces and annealed at 1173 K for 24 h in vacuum quartz tubes, then quenched in cool water. The phase purity and crystal structures were identified by X-ray diffraction (XRD) using Cu Kα radiation at room temperature. The MT temperatures of the alloys were determined by magnetization measurements using a vibration sample magnetometer (VSM).

3. Results and discussion

Fig. 1 shows the XRD patterns of $Ni_{44}Mn_{45}Sn_{10}R$ (R = Al, Ga, In and Sn) alloys at room temperature. The diffraction peaks in the samples were indexed. All the peaks correspond to the Heusler $L2_1$ cubic structure, which indicates that all the samples are in austenitic phase and the MT temperatures are below room temperature. The inset of Fig. 1 shows the enlarged (2 2 0) peaks of the alloys. It is clearly seen that the peak position shifts towards high angles in an order from Sn to In, Al and Ga, indicating cell volume decreases in varying degrees due to the smaller ionic radius of Al, In and Ga compared to Sn. The calculated lattice constants and cell volumes for $Ni_{44}Mn_{45}Sn_{10}R$ (R = Al, Ga, In and Sn) alloys are listed in Table 1.

Fig. 2 shows the temperature dependence of magnetization $M(T)$ curves for $Ni_{44}Mn_{45}Sn_{10}R$ (R = Al, Ga, In and Sn) alloys. The measurements have been performed in an applied field of 1 kOe upon heating and cooling. Both the data from heating and cooling for all samples undergo three successive transitions. As the temperature increases, the samples undergo multiple transitions: (i) ferromagnetic (FM)–paramagnetic (PM) transition at Curie temperature of martensitic phase; (ii) from a low magnetic martensitic state to the FM austenitic phase between A_s and A_f; and (iii) from the FM austenitic to a PM austenitic phase at the Curie temperature of the austenitic phase. Thermal hysteresis on the structural transition between the heating and cooling curves is due to its first-order transition nature. The characteristic temperatures of phase transition (M_s, M_f, A_s and A_f) in $Ni_{44}Mn_{45}Sn_{10}R$ (R = Al, Ga, In and Sn) alloys, determined from the $M(T)$ curves, are listed in Table 1. It can be found obviously that the MT temperatures of the alloys decrease for In doping while increase for Al and Ga doping.

It has been reported that in Heusler alloys the phase stability and transition can be explained by band model [19–21]. In these alloys, if the Fermi surface just touches the (1 1 0) Brillouin zone boundary, the bcc $L2_1$ crystal structure (austenitic phase) is stabilized [19]. Increasing the valence electron concentration in the structure will result in the overlap of Fermi surface and Brillouin zone boundary, then the electrons above the Fermi level will move to the corner states of the Brillouin zone. Due to the excessive increasing of energy, the lattice will distort to minimize the free energy, which leads to the formation of the martensitic phase [20]. On the other hand, smaller radius elements doping will decrease the cell volume and result in a stronger hybridization between Ni and Mn [21], which lead to the increase of the density of states (DOS) near Fermi level and induce the material to undergo martensitic transition, based on the above analysis, it can be concluded that valence electron concentration and cell volume are two main factors influencing the MT temperatures, i.e., increasing the valence electron concentration or decreasing the cell volume will result in higher MT temperatures.

Since all the MT temperatures have the same variation tendency, as a representative, the variation of martensite start temperature M_s with e/a and cell volume are shown in Fig. 3(a) and (b) respectively. Owing to fewer electrons in Al, Ga and In compared with Sn, the $Ni_{44}Mn_{45}Sn_{10}R$ (R = Al, Ga and In) alloys have smaller value of e/a as well as smaller cell volume compared with $Ni_{44}Mn_{45}Sn_{11}$ alloy. We can find that the MT temperatures do not increase or decrease monotonously with the variation of e/a and cell volume respectively. There is a competing effect on the MT temperatures between e/a and cell volume, and the dominating effect decides the shifts of MT temperatures. In the $Ni_{44}Mn_{45}Sn_{10}R$ (R = Al, Ga and In) alloys system, the e/a effect plays the leading role in case of In doping while cell volume effect plays the leading role in case of Al and Ga doping. Hence, neither e/a or cell volume effect can explain the variations of MT temperatures by itself.

Actually, the radius of the Fermi ball, k_F, is a function of the density of valence electrons (n) only. The increase of n will result in the increase of k_F and then the energy of system, which leads to phase transition. Therefore, the density of valence electrons can be used to analyze the shifts of MT temperatures. Electron density n can be described as a function of valence electron concentration e/a and cell volume of austenite. This relationship can be expressed as follows:

$$n = \frac{(e/a) \cdot N}{V_{\text{cell}}} \quad (1)$$

Table 1
The values of lattice constant (a_r) and cell volume V_{cell} of austenite at room temperature, martensite start temperature M_s, martensite finish temperature M_f, austenite start temperature A_s, austenite finish temperature A_f, valence electron concentration e/a and electron density n for $Ni_{44}Mn_{45}Sn_{10}R$ (R = Al, Ga, In and Sn) alloys.

R	a_r (Å)	V_{cell} (Å^3)	M_s (K)	M_f (K)	A_s (K)	A_f (K)	e/a	Electron density, n (/nm^3)
Sn	5.9972	215.7	245.7	225.6	234.5	252.4	7.99	592.68
In	5.9958	215.55	243	223.2	236.3	250.4	7.98	592.35
Al	5.9918	215.12	257.9	246.9	246.9	260.2	7.98	593.53
Ga	5.9891	214.82	267.7	252.9	252.9	272.5	7.98	594.36

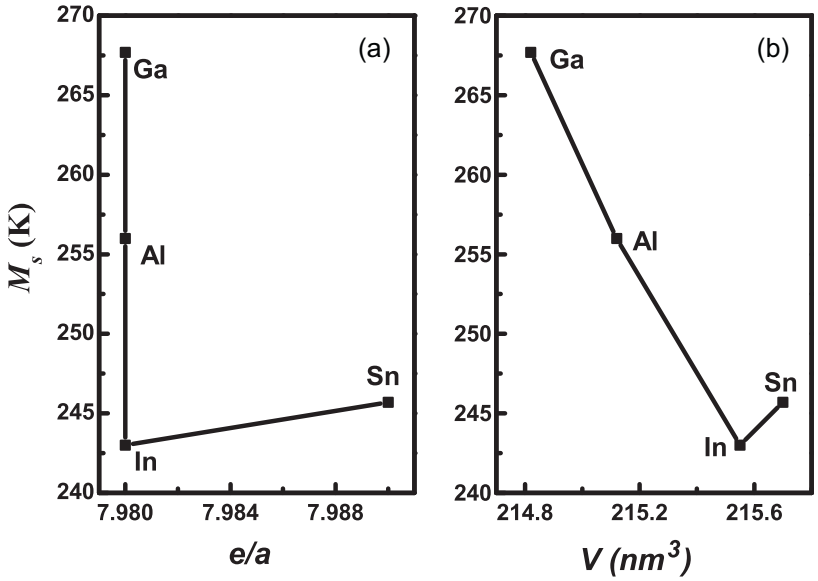

Fig. 3. The variation of martensite start temperature M_s with e/a (a) and cell volume (b).

where N is the average number of atoms contained within a unit cell. As for $Ni_{44}Mn_{45}Sn_{10}R$ (R = Al, Ga, In and Sn) alloys, N is equal to 16. The values of n are listed in Table 1. It should be noted that only the simple alkali metals have a spherical Fermi surface. As for transition metals, and the more complex compounds like Ni–Mn based alloys, their Fermi surface may be substantially different from the sphere. Therefore, the proposed method for determining the density of valence electrons is quite approximate, though, and apparently it can be used for evaluation.

Fig. 4 shows the variations of MT temperatures with n in $Ni_{44}Mn_{45}Sn_{10}R$ alloys. It is clearly that the MT temperatures are very sensitive with n and increase with the increasing of n almost linearly. We have also investigated the relation of MT temperatures and electron density in $Ni_{43}Mn_{46}Sn_{11-x}Ge_x$ alloys of Ref. [17], and the result is very consistent with the rule of this paper. So, combining the effect of valence electron concentration and size factor, the electron density might be a more appropriate factor to describe the shifts of MT temperatures.

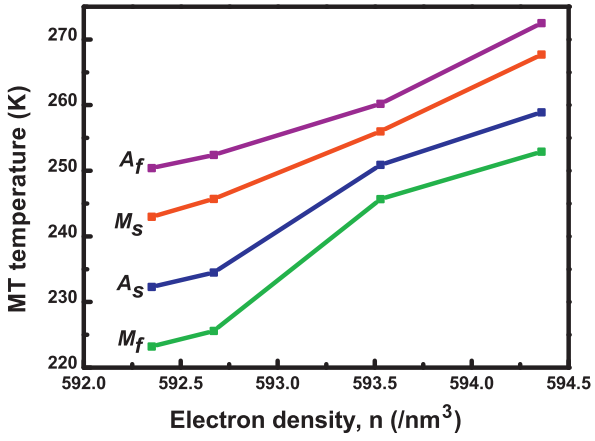

Fig. 4. The variations of MT temperatures with electron density.

4. Conclusion

In summary, we investigated the effect of Al, Ga and In doping on the structure and martensitic transition in $Ni_{44}Mn_{45}Sn_{11}$ alloys. The results indicated that there is a competing effect on the MT temperatures between valence electron concentration and size factor. Considering the size factor and electron concentration together, the MT temperatures increase with the increasing of electrons density, which means the electron density might be a more appropriate factor to describe the shifts of MT temperatures.

Acknowledgements

The authors thank the Natural Science Foundation of China (Grant Nos. 10774040 and 10911120055/A0402), the Ministry of Education of P. R. China (Supported by Program for New Century Excellent Talents in University, No. NCET-08-0674) and the joint Chinese-Russian Project (Grant No. 08-02-92205) for their financial supports.

References

[1] K. Ullakko, J.K. Huang, C. Kantner, R.C. O'Handley, V.V. Kokorin, Appl. Phys. Lett. 69 (1996) 1966.
[2] Y. Sutou, Y. Imano, N. Koeda, T. Omori, R. Kainuma, K. Ishida, K. Oikawa, Appl. Phys. Lett. 85 (2004) 4358.
[3] K. Koyama1, K. Watanabe1, T. Kanomata, R. Kainuma, K. Oikawa, K. Ishida, Appl. Phys. Lett. 88 (2006) 132505.

[4] R. Kainuma, Y. Imano, W. Ito, Y. Sutou, H. Morito, S. Okamoto, O. Kitakami, K. Oikawa, A. Fujita, T. Kanomota, K. Ishida, Nature (London) 439 (2006) 957.
[5] A.M. Aliev, A.B. Batdalov, I.K. Kamilov, V.V. Koledov, V.G. Shavrov, V.D. Buchelnikov, J. García, V.M. Prida, B. Hernando, Appl. Phys. Lett. 97 (2010) 212505.
[6] V. Recarte, J.I. Perez-Landazabal, S. Kustov, E. Cesari, J. Appl. Phys. 107 (2010) 053501.
[7] B.M. Wang, L. Wang, Y. Liu, B.C. Zhao, Y. Zhao, Y. Yang, H. Zhang, J. Appl. Phys. 106 (2009) 063909.
[8] A.K. Pathak, I. Dubenko, C. Pueblo, S. Stadler, N. Ali, Appl. Phys. Lett. 96 (2010) 172503.
[9] L.S.S. Chandra, M.K. Chattopadhyay, V.K. Sharma, S.B. Roy, Phys. Rev. B 81 (2010) 195105.
[10] T. Krenke, M. Acet, E.F. Wassermann, X. Moya, L. Manosa, A. Planes, Phys. Rev. B 72 (2005) 014412.
[11] Z.D. Han, D.H. Wang, C.L. Zhang, H.C. Xuan, B.X. Gu, Y.W. Du, Appl. Phys. Lett. 90 (2007) 042507.
[12] N.V.R. Rao, V. Chandrasekaran, K.G. Suresh, J. Appl. Phys. 108 (2010) 043913.
[13] Z. Li, C. Jing, H.L. Zhang, Y.F. Qiao, S.X. Cao, J.C. Zhang, L. Sun, J. Appl. Phys. 106 (2009) 083908.
[14] A.K. Nayak, K.G. Suresh, A.K. Nigam, J. Appl. Phys. 107 (2010) 09A927.
[15] Z.H. Liu, S. Aksoy, M. Acet, J. Appl. Phys. 105 (2009) 033913.
[16] S. Aksoy, T. Krenke, M. Acet, E.F. Wassermann, X. Moya, L. Manosa, A. Planes, Appl. Phys. Lett. 91 (2007) 241916.
[17] Z.D. Han, D.H. Wang, C.L. Zhanga, H.C. Xuan, J.R. Zhang, B.X. Gua, Y.W. Du, Mater. Sci. Eng. B 157 (2009) 40.
[18] V.K. Sharma, M.K. Chattopadhyay, S.B. Roy, J. Phys. D: Appl. Phys. 43 (2010) 225001.
[19] J. Smit, J. Phys. F: Met. Phys. 8 (1978) 2139.
[20] V.A. Chernenko, Scr. Mater. 40 (1999) 523.
[21] D.N. Lobo, K.R. Priolkar, P.A. Bhobe, D. Krishnamurthy, S. Emura, Phys. Lett. Appl. 96 (2010) 232508.